EASR

Engineering and Applied Science Research

https://www.tci-thaijo.org/index.php/easr/index

Published by the Faculty of Engineering, Khon Kaen University, Thailand

Mean atmospheric temperature model estimation for GNSS meteorology using AIRS and AMSU data

Rata Suwantong[1)], Panu Srestasathiern[1)], Chalermchon Satirapod*[2)], Shi Chuang[3)] and Chaiyaporn Kitpracha[2)]

[1)]Geo-informatics and Space Technology Development Agency (GISTDA), Bangkok 10210, Thailand
[2)]Department of Survey Engineering, Faculty of Engineering, Chulalongkorn University, Bangkok 10330, Thailand
[3)]GNSS Research and Engineering Center, Wuhan University, China

Received April 2016
Accepted June 2016

Abstract

In this paper, the problem of modeling the relationship between the mean atmospheric and air surface temperatures is addressed. Particularly, the major goal is to estimate the model parameters at a regional scale in Thailand. To formulate the relationship between the mean atmospheric and air surface temperatures, a triply modulated cosine function was adopted to model the surface temperature as a periodic function. The surface temperature was then converted to mean atmospheric temperature using a linear function. The parameters of the model were estimated using an extended Kalman filter. Traditionally, radiosonde data is used. In this paper, satellite data from an atmospheric infrared sounder, and advanced microwave sounding unit sensors was used because it is open source data and has global coverage with high temporal resolution. The performance of the proposed model was tested against that of a global model via an accuracy assessment of the computed GNSS-derived PWV.

Keywords: Precipitable Water Vapour (PWV), Global Navigation Satellite System (GNSS), Mean atmospheric temperature, Atmospheric Infrared Sounder (AIRS), Advanced Microwave Sounding Unit (AMSU)

1. Introduction

Physically, Precipitable Water Vapour (PWV) is referred to the amount of liquid water from water vapor condensation. Particularly, it is measured as the height of condensed water per unit area in vertical direction or an atmospheric column. The amount of PWV depends on the location on earth. For example, the amount of PWV at the equator is greater than that of PWV near the poles [1].

Since it is a significant factor for moisture and latent heat transportation [2], it is therefore a crucial information for climate studies, or disaster monitoring. For example, the monitoring of PWV was applied for flash flood prediction [3], and extreme rainfall events [2, 4]. Furthermore, the PWV is a crucial information for generating reliable weather forecast [5-6]. In other words, accurate PWV information is important for numerical weather prediction.

A popular approach for PWV estimation is the use of Continuously Operating Reference Stations (CORS) network [5, 7-9]. The CORS network is a network of GNSS stations that are setup to cover a large area and continuously receive the GNSS signals. Hence, high temporal resolution data covering a large area can be obtained. Namely, CORS network can provides data for continuous, accurate, all-weather, real-time PWV estimation. The atmospheric information is contained in the GNSS signal in terms of the signal propagation delay, particularly the Zenith Total Delay (ZTD) which can be extracted by the Precise Point Positioning (PPP) technique. PWV is then extracted from ZTD.

The conversion from ZTD to PWV is a function of the water vapor weighted mean atmospheric (tropospheric) temperature T_m. The difficulty is that T_m cannot be measured directly in realtime. An indirect measurement is to convert the air surface temperature T_s, which is measured at or near the GNSS receiver, to T_m. In literature, there exists many global model for T_m - T_s conversion [5, 10-11]. However, a local T_m - T_s conversion model can provide GNSS-derived PWV with better accuracy [2].

Traditionally, the estimation of local T_m-T_s conversion models uses radiosondes and ground-based Microwave Radiometers (MWR) data. Although radiosondes and MWR can provide accurate data for meteorology applications, the radiosonde network is expensive to operate. Namely, the obtained data has a sparse spatial coverage at low temporal frequency [12].

To achieve better coverage both temporally and spatially at smaller cost, in this paper, it is proposed to use the data from the Atmospheric Infrared Sounder (AIRS), and the Advanced Microwave Sounding Unit (AMSU) installed on NASA's Aqua satellite to derive a local T_m and T_s relationship model. To formulate the relationship

*Corresponding author. Tel.: +66 2218 6651 5 ext 312
Email address: rata@gistda.or.th, panu@gistda.or.th, chalermchon.s@chula.ac.th*, shi@whu.edu.cn, chaiyaporn.k@chula.ac.th
doi: 10.14456/easr.2017.8

mathematically between T_m and T_s, the triply modulated cosine was adopted to model T_s as a periodic function. The surface temperature is then converted to T_m by a linear function. The parameters of the model are estimated using extended Kalman filter.

The rest of this paper is organized as follows. In Section 2, the method for extracting PWV from GNSS observations is discussed. In Section 3, AIRS and AMSU satellite data preparation, and T_m and T_s relationship formulation will be presented. The extended Kalman filter technique for model parameter estimation will be explained in Section 4. The experimental results of the parameters for the local Tm relation and the accuracy of the GNSS PWV derived using the global and local models will be studied in Section 5. The concluding remarks will be presented in the last section.

2. Precipitable water vapor estimation using satellite geodesy

A. Precipitable water vapour computation from the ZTD

In [13], Saastamoinen studied the effect of troposphere causing the delay on microwave propagation. Such delay depends on the temperature, the pressure, and the water vapor. These factors can change the reflective index along the signal traveling path. The variation of reflective index yield the delay in the signal propagation. Such delay is hence called *tropospheric delay*.

In the seminal work by Bevis et al. [5], the tropospheric delay of GPS signal was used to infer quantity of water vapor which is called *Precipitable Water Vapor* (PWV). Particularly, it is referred to the amount of water vapor in vertical direction after condensation in millimeter unit.

PWV can be calculated from the Zenith Total Delay (ZTD) which can be obtained using GNSS data processing technique called Precise Point Positioning (PPP). ZTD can be decomposed into two parts. The first one is the Zenith Hydrostatic Delay (ZHD) which is contributed by dry air and the nondipole component of water vapor. The second one is the Zenith Wet Delay (ZWD) which is associated solely with the dipole component of the water vapor in the atmosphere. Mathematically, ZTD can be simply formulated as $ZTD = ZHD+ZWD$ or equivalently, $ZWD = ZTD–ZHD$.

To extract the ZWD component from ZTD, the ZHD is modeled as the function of pressure, latitude, and height [13]:

$$ZHD = \frac{2.2768P_s}{1 - 0.00266\cos(2\emptyset) - 0.00000028H}, \quad (1)$$

where P_s is the air surface pressure in bar, $\emptyset$ the latitude of the receiver, and H the height above the ellipsoid in meter. After the ZWD is extracted, it can then be recast to PWV by:

$$PWV = \Pi \cdot ZWD. \quad (2)$$

The coefficient Π is given by equation:

$$\Pi = \frac{10^{-6}}{R_w\left(k_2' + \frac{k_3}{T_m}\right)} \quad (3)$$

where k_2' and k_3 are empirical coefficients. In this paper, the values are k_2' = 0.221K/Pa, k_3 = 3739K/Pa^2. R_w = 461.525J/(kg·K) is a specific gas constant of water vapor. T_m is the water vapor-weighted mean tropospheric temperature which is also called the mean tropospheric temperature in *K*. Although the mean tropospheric temperature depends on the temperature profile in troposphere, it can be estimated using average of the surface temperature at the GNSS receiver.

It can be observed that the conversion from ZWD to PWV is a function of T_m which is difficult to be estimated especially in realtime. One of the solution is to estimate T_m using surface temperature T_s which is much easier to obtain. That is, T_m is modeled as a function of T_s.

B. Existing tropospheric mean temperature models

A simple mathematical formulation is the linear function which can be simply expressed as:

$$T_m = aT_s + b, \quad (4)$$

where a and b are empirical coefficients given in many versions by different sources. The variation of such parameters is associated with location, height, season and weather. In [5], the relation between T_m and T_s is formulated as:

$$T_m = 0.72T_s + 70.2 \quad (5)$$

for the region between Alaska and Florida. However, It was mentioned in [11] that this parameters can be used globally.

Mendes et al. [10] estimated the parameters a and b using radiosonde data. Particularly, the linear function (4) was fitted to 32,500 radiosonde profiles from 50 stations covering 62°S–83°N. The fitted model is:

$$T_m = 0.789T_s + 50.4. \quad (6)$$

In stead of using the linear function, Schueler et al. proposed an alternative model called mixed harmonic/surface temperature model at the request day of year (DoY):

$$T_m = \bar{T}_m + \tilde{T}_m cos\left(2\pi\frac{DoY - DoY_w}{365.25}\right) + q_T T_s, \quad (7)$$

where

T_m	mean temperature at day DoY
$\bar{T}_m$	the average of T_m
$\tilde{T}_m$	the amplitude of the annual cycle of T_m
DoY	the day of year
DoY_w	the day of the year for maximum winter, equal to 28 for the Northern Hemisphere and to 211 for the Southern Hemisphere
q_T	is an amplifier-weighting term for the T_s

Note that $\bar{T}_m$, $\tilde{T}_m$ and q_T are specific for each station. It can be observed that this model is just an combination of harmonic function of T_m and a linear function of T_s. The global linear surface temperature model was also derived:

$$T_m = 0.647T_s + 86.9, \quad (8)$$

which is different from the models given by Bevis et al. [5] and Mendes et al. [10] because those models were derived locally.

The important of accurate T_m for estimating PWV was pointed out by in [2]. Namely, T_m is the largest source of error in PWV estimation. Moreover, local T_m model should be used to obtain accurate GNSS derived PWV [7]. Generally, the coefficients of each meteorological

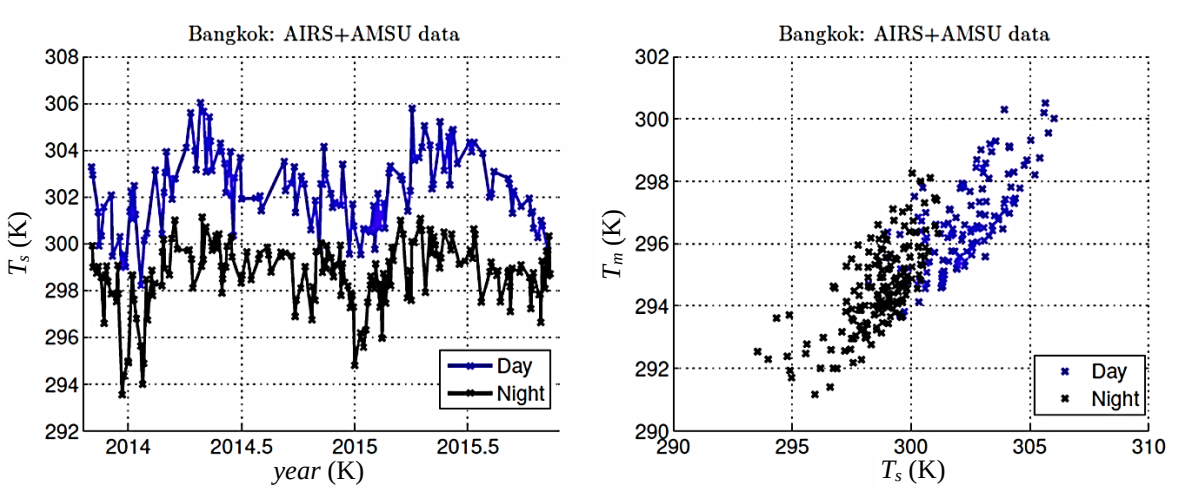

Figure 1 Air surface temperature in time in year (left) and correlation between the mean tropospheric temperature and the air surface temperature (right), both for Bangkok from November 2013 to November 2015.

in T_m - T_s relation are estimated using radiosonde data. However, the obtained data does cover a large area and the operation cost is very costly.

To address this issue, in this paper, an alternative method for estimating the parameters of T_m and T_s relation is proposed. That is, the satellite data from the Atmospheric Infrared Sounder (AIRS) and the Advanced Microwave Sounding Unit (AMSU) equipped on Aqua satellite are used to derive the relation between T_m and T_s. The advantage of this approach is that the data is free of charge. Moreover, this approach is suitable for the areas that radiosonde data is not available.

Table 1 The data layers used for deriving T_m model

Data layer	Description
pressStd	pressure level for atmospheric temperature profile
pressH2O	pressure level for water vapor profile
TAirStd	atmospheric temperature profile
H2OMMRLevStd	mixing ratio profile
TSurfAir	air surface temperature

3. Mean tropospheric temperature retrieval from satellite data

A. AIRS and AMSU data

AIRS and AMSU are sensors equipped on NASA's Aqua satellite. It was designed to have 2 days revisiting time. The global coverage is thus possible with high temporal frequency. The data from AIRS and AMSU are processed together to have level 2 standard product called AIRX2RET where version 6 is the latest version as of April, 2016. The processed data is stored in Hierarchical Data Format (HDF) and can be download from NASA's website. In one HDF file, there are many data layers. The data layers used in this paper are listed in Table 1. For further information on the AIRX2RET products, the readers are referred to [14].

In this paper, the region of interest in Thailand was used in the study. Since Aqua passes Thailand two times around 2 and 13 o'clock local time daily, the local T_m models for day and night are thus possible to be derived separately.

The processed AIRS and AMSU data provide atmospheric temperature profile at 28 standard pressure levels from bottom atmosphere to the top, while the water vapor profile is provided at 15 pressure levels. Furthermore, the pressure level for water vapor profile is the same as the firs 15 pressure levels for atmospheric temperature profile.

In [15], the accuracies of AIRS and AMSU products i.e., atmospheric temperature and water vapor were evaluated. That is, the accuracy of estimated atmospheric temperature is about 1 K for 1-km resolution. For water vapor estimation, the uncertainty is about 15% for 2-km resolution.

B. Computing mean tropospheric temperature from AIRS and AMSU

Given the water vapor partial pressure e_i and the air temperature T_i at the pressure level i, the mean atmospheric temperature can be computed as the following:

$$T_m = \sum \frac{e_i}{T_i} / \sum \frac{e_i}{T_i^2} \tag{9}$$

It can be observed that this formulation is the weighted harmonic mean of the air temperature T_i with weight $\frac{e_i}{T_i}$.

To compute water vapor partial pressure e_i at level i, the mixing ratio at level i (w_i) is taken into account. That is, the total pressure level is converted to the water vapor partial pressure:

$$e_i = \frac{w_i}{w_i + \varepsilon} p_i, \tag{10}$$

where p_i is the total pressure level. ε is ratio between the molecular weight of water M_w and the apparent molecular weight of dry air M_d i.e., $\varepsilon = \frac{M_w}{M_d} = 0.622$. It must be aware that the mixing ratio must be scaled by 10^{-3} before computing (10) because the unit of the mixing ratio from AIRS is g/kg.

C. Mean tropospheric temperature and air surface temperature models

In order to explain the rational behind the temperature model proposed in this paper, in Figure 1, the temperature data for Bangkok, Thailand from November 2013 to

November 2015 were illustrated. It can be observed that T_s is a periodic function of time with a period of 1 year. Furthermore, T_m and T_s show a linear relationship. By combining these two observations, it is therefore hypothesized that the periodicity of T_m is induced from T_s through linear relationship. This hypothesis is different from the harmonic model proposed in [11] as shown in (7). That is, the T_m itself in (7) is a periodic function.

To formulate the T_m and T_s relationship, T_s is first modelled as a periodic function:

$$T_{s_k} = \mu_k + A_k \sin\left(2\pi \frac{DoY}{365.25} + \emptyset_k\right) \quad (11)$$

where μ_k, A_k, $\emptyset_k$ are the mean, the amplitude and the initial phase of the sine function at instant k respectively. This periodic function is also known as triply (mean, phase, and amplitude) modulated cosine function which is popular for modelling the time series of satellite data [16]. T_s is then converted to T_m by a linear function:

$$T_{m_k} = aT_{s_k} + b \quad (12)$$

The parameters a, b, μ_k, A_k, and $\emptyset_k$ are then estimated independently to obtain a local T_m model for the area of interest.

4. Deriving the mean tropospheric temperature model using the Extended Kalman filter

A. State and measurement definitions

To estimate the parameters of T_m and T_s relationship expressed in (11) and (12), the sequential parameter estimation method called Extended Kalman Filter (EKF) is adopted and the data from AIRS and AMSU is used as measurement.

According to (11) and (12), the state vector x_k containing the parameters to be estimated at instant k is expressed as:

$$\mathrm{x}_k = [a_k\ b_k\ \mu_k\ A_k\ \emptyset_k]^T. \quad (13)$$

To define the state equation for EKF, it is assumed that the state vector does not change much from the previous instant. The state vector is thus propagated by:

$$\mathrm{x}_k + 1 = f(\mathrm{x}_k) + \mathrm{w}_k = \mathrm{x}_k + \mathrm{w}_k, \quad (14)$$

Where $\mathbf{w}_k \sim \mathcal{N}(\mathbf{0}, \mathtt{Q})$ is a zero-mean white Gaussian process noise with covariance matrix $\mathtt{Q}$. The function $f(\cdot)$ is called the state equation.

The measurement vector y_k at instant k is therefore the mean atmospheric and surface temperatures i.e., $\mathrm{y}_k = \left[T_{m_k}\ T_{s_k}\right]^{\mathrm{T}} + \mathrm{v}_k$ where $\mathbf{v}_k \sim \mathcal{N}(0, R)$ is a zero-mean white Gaussian measurement noise with covariance matrix R. Remind that T_{s_k} and T_{m_k} are retrieved from AIRS and AMSU at instant k. Therefore, by combining (11) and (12), the measurement vector can be expressed as a function of the state as:

$$\mathrm{y}_k = h(\mathrm{X}_k) + \mathrm{v}_k \quad (15)$$

$$= \begin{bmatrix} a_k \left(\mu_k + A_k \sin\left(2\pi \frac{DoY}{365.25} + \emptyset_k\right)\right) + b_k \\ \left(\mu_k + A_k \sin\left(2\pi \frac{DoY}{365.25} + \emptyset_k\right)\right) \end{bmatrix}$$

The function h is called the measurement. Given both state and measurement equations, the parameters of the T_m and T_s relationship can then be estimated using EKF technique.

B. Extended Kalman Filter equations and parameter initialization

a) EKF Equations: To estimate the state vector, the EKF algorithm traditionally consists of two steps i.e., prediction and update as follows [17]:

Prediction:*

$$\hat{\mathrm{x}}_k^- = f(\hat{\mathrm{x}}_{k-1}), \mathrm{P}_k^- = \mathrm{Q}_{k-1} + \hat{\mathrm{F}}_{k-1}\mathrm{P}_{k-1}\hat{\mathrm{F}}_{k-1}^T, \hat{\mathrm{F}}_{k-1} = \left.\frac{\partial f}{\partial \mathrm{x}}\right|_{\mathrm{x}=\hat{\mathrm{x}}_{k-1}}$$

Update:

$$\hat{\mathrm{x}}_k = \hat{\mathrm{x}}_k^- + \mathrm{K}_k\left(\mathrm{y}_k - h(\hat{\mathrm{x}}_k)\right), \mathrm{S}_k = \hat{\mathrm{H}}_k P_k^- \hat{\mathrm{H}}_k^T + \mathrm{R}_k$$
$$\mathrm{K}_k = \mathrm{P}_k^- \hat{\mathrm{H}}_k^T \mathrm{S}_k^{-1}, \mathrm{P}_k = \mathrm{P}_k^- - \mathrm{K}_k \mathrm{S}_k \mathrm{K}_k^T, \hat{\mathrm{H}}_k = \left.\frac{\partial h}{\partial \mathrm{x}}\right|_{\mathrm{x}=\hat{\mathrm{x}}_k}, \quad (16)$$

where $\hat{\mathrm{x}}_k^-$ is the a priori estimate at instant k, P_k^- is the a priori estimation error covariance matrix, $\hat{\mathrm{x}}_k$ is the a posteriori estimate, and P_k is the a posteriori error covariance matrix.

b) Parameter initialization: Since EKF is an iterative process, the state vector $\hat{\mathrm{x}}_0^-$ (13) or parameters must be initialized. The mean μ_k can be initialized by using the average of all T_s measurements. The initial A_k and phase $\emptyset_k$ can be computed using Fourier transformation of the T_s time series. That is, the magnitude and phase of the first harmonic are used as the initial values for A_k and $\emptyset_k$. The parameters of global T_m-T_s models can then be used to initialize a_k and b_k e.g., the parameters of (8).

The initial a priori error covariance matrix P_0^- which represents the confidence in the a priori initial state is chosen such that

$$\mathrm{P}_0^- = \mathbf{diag}\,(1\ \ 20\ \ 5\ \ 5\ \ 5 \cdot \pi/180)^2. \quad (17)$$

To model the process noise, a and b are assumed to be constant as done for the global models in (5), or (8). That is, the process noise on a and b are supposed to be zero. The process noise covariance matrix $\mathtt{Q}$ is then:

$$\mathtt{Q} = \mathbf{diag}\,(0\ \ 0\ \ 0.5\ \ 0.1\ \ 0.1 \cdot \pi/180)^2. \quad (18)$$

Regarding the analysis in [15], the accuracy for atmospheric and surface temperatures is about 1 K for 1 km resolution, the measurement noise covariance matrix is chosen as

$$\mathrm{R} = \mathbf{diag}\,(0.5\ \ 0.5)^2. \quad (19)$$

By the nature of EKF, a and b parameters are updated at each iteration. However, the estimated a and b at the final instant will be used as the local T_m model. The rationale for selecting a and b parameters is that a and b parameters are assumed to converge as the time goes by.

5. Experimental results

A. Estimated parameters for T_m and T_s models

To evaluate the performance of the proposed T_m model estimation method, the experiment was conducted using the AIRS and AMSU data from September, 2010 to September,

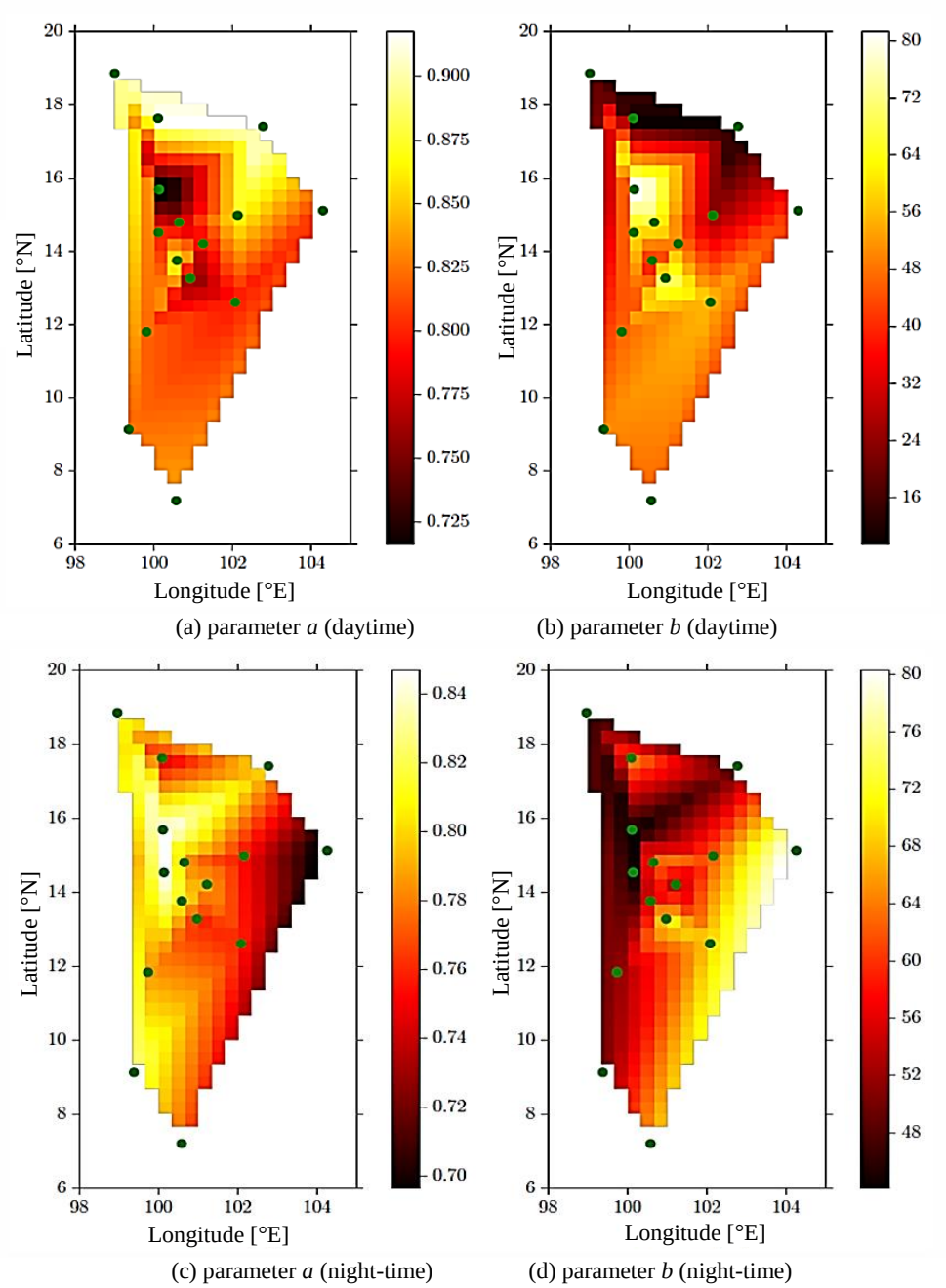

Figure 2 The estimated parameters *a* and *b* for **night time**. The positions of CORS stations are plotted with green dots.

2015. Particularly, the T_m and T_s data at the CORS station was used.

The estimated $\hat{a}$ and $\hat{b}$ parameters in the T_m and T_s relationship (4) at each CORS station for day and night times are illustrated in Figure 2. The parameters *a* and *b* at each CORS stations, which are shown as green dots on the plot, were first estimated. The parameters for other positions were then calculated by bi-linear interpolation technique. It can be observed that the parameters *a* and *b* depend on the spatial location. Moreover, they are also function of time.

To evaluate the accuracy of the obtained parameters from the proposed method, T_m and T_s obtained from AIRS and AMSU respectively at the CORS station in Bangkok is plotted along with global T_m models (5), (6), (8), and the derived local T_m models are plotted in Figure 3 where it can be observed that the local models fit more the AIRS and AMSU observations than the global models.

B. Accuracy of GNSS PWV using Local and Global models

To demonstrate the efficiency of the estimated *a* and *b* parameters i.e., local T_m model, the accuracy of GNSS-derived PWV was used. That is, the PWVs extracted from GNSS using local and global T_m models i.e., (6) were compared with a reference one. Traditionally, PWV obtained from the microwave radiometer is utilized. An alternative is to use satellite imagery i.e., AIRS, and AMSU as reference. In [18], it was reported that the PWV retrievals using AIRS, and AMSU have a strong agreement with the microwave radiometer with a bias of -0.233 mm and root mean squared

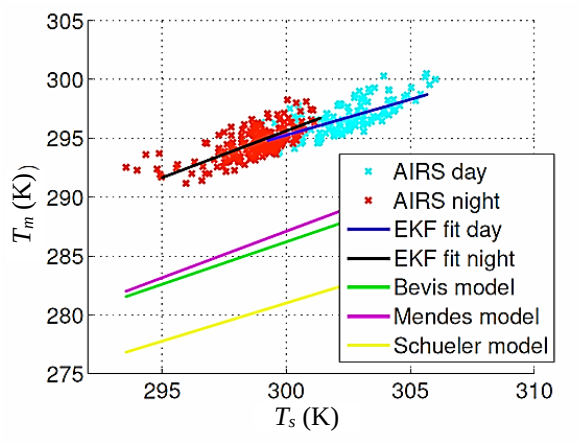

Figure 3 T_m and T_s from AIRS and AMSU along with global T_m models and the derived local T_m models at Bangkok CORS station.

Table 2 t-statistics for bias detection, where the error is $PWV_{GNSS} - PWV_{AIRS}$

T_m model	Mean error [K]	Standard error of of the mean difference [K]	t-statistics
Local model	0.199	0.786	0.253
Global model (6)	-1.063	0.764	-1.391

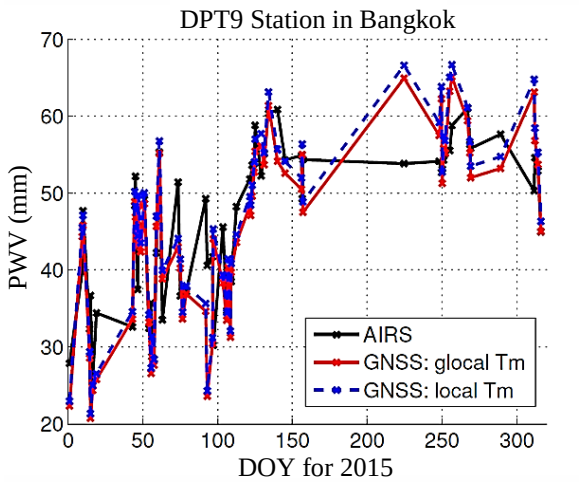

Figure 4 PWV derived from GNSS observations using the global T_m model (in red) and that derived using the local BKK T_m model (in blue) compared with the PWV from AIRS and AMSU (in black).

error of 2.103 mm in day time in tropical area from September 2002 through August 2008.

In this experiment. GNSS observations from the CORS own by the Department of Public Works and Town & Country Planning (DPT) of Thailand from January 2015 to November 2015 were utilized. The PPP technique implemented in the PANDA software from Wuhan university was used for data processing i.e. ZTD extraction, The surface temperature at the CORS station was used to compute T_m using local, and global models. The obtained T_m was then used to compute coefficient Π in (3) for PWV extraction. In Figure 4, the time series of estimated PWV using local, and global T_m models together with the PWV from AIRS and AMSU are illustrated.

The efficiency of the estimated T_m model was evaluated by bias detection in PWV computation. The bias detection was performed by single sample *t*-test. Particularly, the hypothesis testing is used to test whether there exists a bias in the GNSS-derived PWV using the local or global models. Therefore, the null hypothesis H_0 , and the alternative hypothesis H_1 were set as H_0: $\bar{e} = 0$ and H_1 : $\bar{e} \neq 0$, where e is the error of GNSS-derived PWV compared with PWV from AIRS and AMSU e.g., $PWV_{GNSS} - PWV_{VAIRS}$. For the two tailed test, the null hypothesis is rejected, if the absolute value of the *t*-statistics is less than the *t* distribution $t_{n-1,\alpha}$, where n is the number of samples and α is the significant level.

In the testing, samples from 64 days were used. The *t*-statistics of error using local and global T_m models in GNSS derived PWV are reported in Table 2. For 2-tailed $\alpha = 0.2$ (90% confidence) and 63 degree of freedom, the critical value for the *t* distribution is about 1.29. Therefore, it cannot be rejected that the GNSS-derived PWV using local T_m model has no bias. In contrast, for the global model, the null hypothesis cannot be accepted. That is, we cannot accept that there is no bias in the GNSS-derived PWV using global model.

Moreover, It can be observed from the mean error of global model that PWV is underestimated because the mean error is less than zeros. Referred to Figure 3, T_m from global model is less than the measured one. This yields the shrinkage in the value of coefficient Π in (3) and the extracted PWV.

6. Concluding remarks

In this paper, the data from AIRS, and AMSU equipped on NASA's Aqua satellite were used to derive a local T_m and T_s relationship. The algorithm utilized for solving the local model parameters was the extended Kalman filter. Air surface temperatures was modeled using the triply modulated cosine because of its periodicity. The surface temperature is then converted to mean atmospheric temperature by a linear function. Traditionally, the radiosonde data is used as measurement. In this paper, the satellite data from atmospheric infrared sounder, and advanced microwave sounding unit sensors was used because it is free of charge and has global coverage and high temporal resolution. The performance of the proposed model was tested against the global model. It was shown that there were no biases in the GNSS-derived PWV using local T_m model. In contrast, using global T_m yielded bias in the PWV estimation.

7. Acknowledgement

The authors would like to thank the GNSS Research Center, Wuhan University of China for kindly providing us the PANDA Software for GNSS data processing. Also, we would like to express our gratitude to the Department of Public Works and Town & Country Planning of Thailand for GNSS observations from their CORS network. Also, we would like to thank Prof. Dr. Allen Huang from the Cooperative Institute for Meteorological Satellite Studies, Space Science and Engineering Center, University of Wisconsin-Madison, for his advice on water vapour retrieval from satellite data.

8. References

[1] Brutsaert W. Hydrology: an introduction. New York: Cambridge University Press; 2005.

[2] Awange JL. Environmental monitoring using GNSS: global navigation satellite systems. New York: Springer-Verlag Berlin Heidelberg; 2012.

[3] Awange J, Fukuda Y. On possible use of GPSLEO satellite for flood forecasting. International civil engineering conference on sustainable development in the 21st century The Civil Engineer in Development; 2003 Aug 12-16; Nairobi, Kenya. p. 12-6.

[4] Wang B, Zhao L, Bai X. The characteristics investigation of ground-based GPS/PWV during the 7.21 extreme rainfall event in beijing. In: Sun J, Liu J, Fan S, Lu X, editors. China Satellite Navigation Conference (CSNC) 2015; 2015 May 13-15; Xian, China. New York: Springer-Verlag Berlin Heidelberg; 2015. p. 563-74.

[5] Bevis M, Businger S, Herring TA, Rocken C, Anthes RA, Ware RH. GPS meteorology: remote sensing of atmospheric water vapor using the global positioning system. J Geophys Res Atmos. 1992;97(D14): 15787-801.

[6] Baker H, Dodson A, Penna N, Higgins M, Offiler D. Ground-based GPS water vapour estimation: potential for meteorological forecasting. J Atmos Sol Terr Phys. 2001;63(12):1305-14.

[7] Sapucci LF. (2014). Evaluation of modeling watervapor-weighted mean tropospheric temperature for GNSSintegrated water vapor estimates in Brazil. J Appl Meteorol Clim. 2014;53(3):715-30.

[8] Alshawaf F, Fersch B, Hinz S, Kunstmann H, Mayer M, Meyer F. Water vapor mapping by fusing InSAR and GNSS remote sensing data and atmospheric simulations. Hydrol Earth Syst Sci. 2015;19(12): 4747-64.

[9] Wilgan K, Rohm W, Bosy J. Multi-observation meteorological and GNSS data comparison with numerical weather prediction model. Atmos Res. 2015;156:29-42.

[10] Mendes V, Prates G, Santos L, Langley R. An evaluation of the accuracy of models for the atmosphere. Proceedings of the 2000 National Technical Meeting of The Institute of Navigation; 2000 Jan 26-28; Anaheim, California. p. 433-8.

[11] Schueler T, P´osfay A, Hein GW, Biberger R. A global analysis of the mean atmospheric temperature for GPS water vapor estimation. Proceedings of 14th International Technical Meeting of Satellite Division of The Institute of Navigation; 2001 Sep 11-14; Utah, USA. p. 2476-89.

[12] Satirapod C, Anonglekha S, Choi YS, Lee HK. Performance assessment of GPS-sensed precipitable water vapor using igs ultra-rapid orbits: a preliminary study in thailand. Eng J. 2010;15(1):1-8.

[13] Saastamoinen, J. Atmospheric correction for the troposphere and stratosphere in radio ranging satellites. In: Soren WH, Armando M, Bernard HC, editors. The use of artificial satellites for geodesy. Washington, DC: American Geophysical Union; 1972. p. 247-51.

[14] Olsen E, Fetzer E, Hulley G, Manning E, Blaisdell J, Iredell L, et al. AIRS/AMSU/HSB version 6 level 2 product user guide. USA: NASA-JPL Tech Rep; 2013.

[15] Divakarla MG, Barnet CD, Goldberg MD, McMillin L M, Maddy E, Wolf W, et al. Validation of atmospheric infrared sounder temperature and water vapor retrievals with matched radiosonde measurements and forecasts. J Geophys Res Atmos. 2006;111(D9):1-20.

[16] Kleynhans W, Olivier JC, Wessels KJ, van den Bergh F, Salmon BP, Steenkamp KC. Improving land cover class separation using an extended kalman filter on modis ndvi time-series data. Geosci Rem Sens Lett IEEE. 2010;7(2):381-5.

[17] Suwantong R. Development of the Moving Horizon Estimator with Pre-Estimation (MHE-PE). Application to Space Debris Tracking during the Re-Entries [PhD dissertation]. French: Sup´elec; 2014.

[18] Bedka S, Knuteson R, Revercomb H, Tobin D, Turner D. An assessment of the absolute accuracy of the atmospheric infrared sounder v5 precipitable water vapor product at tropical, midlatitude, and arctic groundtruth sites: september 2002 through august 2008. J Geophys Res Atmos. 2010;115(D17):1-17.